ISSN 0020-1685, Inorganic Materials, 2018, Vol. 54, No. 7, pp. 724–735. © Pleiades Publishing, Ltd., 2018.
Original Russian Text © T.V. Safronova, V.I. Putlyaev, Ya.Yu. Filippov, T.B. Shatalova, D.O. Naberezhnyi, A.F. Nasriddinov, D.S. Larionov, 2018, published in Neorganicheskie Materialy, 2018, Vol. 54, No. 7, pp. 765–776.

Ceramics Based on Powder Mixtures Containing Calcium Hydrogen Phosphates and Sodium Salts (Na_2CO_3, $Na_4P_2O_7$, and $NaPO_3$)

T. V. Safronova[a], *, V. I. Putlyaev[a], Ya. Yu. Filippov[a], T. B. Shatalova[a], D. O. Naberezhnyi[a], A. F. Nasriddinov[a], and D. S. Larionov[a]

[a] *Moscow State University, Moscow, 119991 Russia*

**e-mail: t3470641@yandex.ru*

Received December 21, 2017

Abstract—Ceramic materials in the Na_2O–CaO–P_2O_5 system have been produced using powder mixtures containing calcium hydrogen phosphates (monetite/brushite: $CaHPO_4$/$CaHPO_4 \cdot 2H_2O$) and sodium salts ($Na_2CO_3 \cdot H_2O$, $Na_4P_2O_7 \cdot 10H_2O$, and $NaPO_3$). These salts were used as precursors to the following high-temperature phases: $Ca_2P_2O_7$, Na_2O, $Na_4P_2O_7$, and $NaPO_3$. The amount of the salts in the powder mixtures was such that the oxide composition of the ceramics corresponded to 10 mol % sodium oxide for each mixture in the Na_2O–CaO–P_2O_5 system. The powder mixtures were prepared using mechanical activation in acetone, which was accompanied by monetite rehydration to brushite. X-ray diffraction characterization showed that, after firing, the phase composition of the ceramics produced from the powder mixtures thus prepared lay in the $Ca_2P_2O_7$–$NaCaPO_4$–$Na_2CaP_2O_7$–$Ca(PO_3)_2$ phase field. The resultant ceramic materials contain biocompatible and bioresorbable phases and can be recommended for bone implant fabrication.

Keywords: synthesis, brushite, monetite, sodium carbonate monohydrate, sodium pyrophosphate decahydrate, sodium polyphosphate, mechanical activation, monetite rehydration, bioceramics, composite, calcium pyrophosphate, rhenanite, sodium calcium double pyrophosphate

DOI: 10.1134/S0020168518070166

INTRODUCTION

The chemical composition of bone tissue, containing hydroxyapatite and a number of biocompatible ions, such as Na^+, K^+, Mg^{2+}, CO_3^{2-}, and SiO_4^{4-} [1, 2], allows one to consider the possibility of creating bone implant materials in not only the CaO–P_2O_5 or CaO–P_2O_5–H_2O system but also systems containing sodium, potassium, magnesium, silicon, and carbon oxides [3, 4]. Materials in oxide systems containing CaO, P_2O_5, and Na_2O have long been the focus of researchers' attention [5–7].

For the development of regenerative methods of treating bone tissue defects, it is necessary to create materials capable of gradually dissolving (resorbing) after implantation. Biocompatible and bioresorbable materials in the Na_2O–CaO–P_2O_5 system may contain the following phases [8–11]: tricalcium phosphate, $Ca_3(PO_4)_2$ (Ca/P = 1.5); calcium pyrophosphate, $Ca_2P_2O_7$ (Ca/P = 1.0); tromelite, $Ca_4P_6O_{19}$ (Ca/P = 0.66); calcium polyphosphate, $Ca(PO_3)_2$ (Ca/P = 0.5); sodium-substituted tricalcium phosphate; sodium rhenanite, $NaCaPO_4$; sodium calcium double pyrophosphate, $Na_2CaP_2O_7$; and phosphate glasses.

Ceramic composites containing the above biocompatible and bioresorbable phases can be produced from both a powder mixture containing direct precursors of the phases of interest and a powder mixture whose components enter into a heterogeneous reaction on heating [11].

The purpose of this work was to prepare resorbable ceramic composite materials in the Na_2O–CaO–P_2O_5 system using powder mixtures containing synthetic powder of calcium phosphates with a calcium/phosphorus molar ratio Ca/P = 1 ($CaHPO_4 \cdot 2H_2O$ and $CaHPO_4$) and different sodium salts ($Na_2CO_3 \cdot H_2O$, $Na_4P_2O_7 \cdot 10H_2O$, and $NaPO_3$). The amount of the sodium salts added to the powder mixtures was such that the sodium oxide content in the Na_2O–CaO–P_2O_5 system was 10 mol %. The compositions to be studied lie on the Na_2O–$Ca_2P_2O_7$, $Na_4P_2O_7$–$Ca_2P_2O_7$, and $NaPO_3$–$Ca_2P_2O_7$ lines. The intended oxide compositions in the Na_2O–CaO–P_2O_5 system fall in the phase field formed by the following compounds: calcium pyrophosphate, $Ca_2P_2O_7$; rhenanite, $NaCaPO_4$; sodium calcium double pyrophosphate, $Na_2CaP_2O_7$; and calcium polyphosphate, $Ca(PO_3)_2$. It is these phases which are expected to enter into the composition of the ceramic material to be produced.

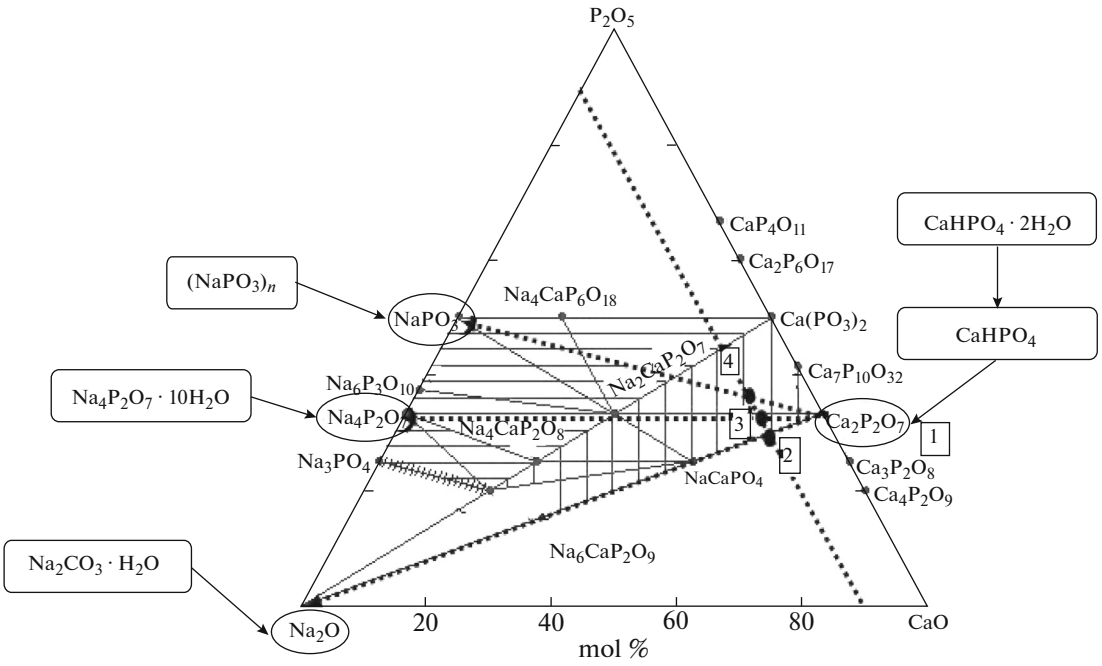

Fig. 1. Na_2O–CaO–P_2O_5 phase diagram showing the intended compositions of ceramics (1–4), high-temperature phases ($Ca_2P_2O_7$, Na_2O, $Na_4P_2O_7$, and $NaPO_3$), and their precursors in the starting powder mixtures.

EXPERIMENTAL

Brushite was synthesized using 1 M aqueous solutions of calcium nitrate ($Ca(NO_3)_2$, Ruskhim, Premium grade, Russian Federation Purity Standard TU 2143-017-77381580-1212) and ammonium hydrogen phosphate ($(NH_4)_2HPO_4$, Sigma Aldrich, puriss. p.a., ≥99.0%) at a calcium/phosphorus molar ratio Ca/P = 1. The amounts of the starting chemicals were calculated according to the reaction (1).

$$Ca(NO_3)_2 + (NH_4)_2HPO_4 + 2H_2O = CaHPO_4 \cdot 2H_2O + 2NH_4NO_3. \quad (1)$$

The ammonium hydrogen phosphate solution was added to the calcium nitrate solution. After the addition of ammonium hydrogen phosphate, the resultant suspension was stirred on a magnetic stirrer at room temperature with constant stirring for 15 min. Next, the synthesis product was separated from the mother liquor in a Buchner funnel. After the synthesis, the precipitate was placed in plastic containers and dried in air for a week and then in a drying oven at a temperature of 40°C for 2 h. The oxide compositions of the ceramic materials produced in the Na_2O–CaO–P_2O_5 system are indicated in Fig. 1 and the intended composition of the powder mixtures under investigation, containing monetite and sodium salts, is specified in Table 1. The composition of the starting powder mixtures was chosen with allowance for thermal analysis data for their components. The powder mixtures containing monetite and sodium salts (Table 2) were disaggregated and homogenized under acetone (Russian Federation Standard GOST 2603-79) by grinding in a planetary mill for 15 min, using agate vials and zirconia grinding media. The sodium salts used were sodium carbonate monohydrate ($Na_2CO_3 \cdot H_2O$, Sigma Aldrich, puriss. p.a., ≥99.5%), sodium pyrophosphate decahydrate ($Na_4P_2O_7 \cdot 10H_2O$, Sigma Aldrich, puriss. p.a., ≥99.5%), and sodium polyphosphate ($(NaPO_3)_n$, Sigma Aldrich). Acetone was used as a disaggregation/homogenization medium. The powder-to-ball weight ratio was 1 : 5. After disaggregation and homogenization, the powders were dried in air at room temperature for 2 h. Next, the powders were passed through a sieve with a nominal aperture size of 200 μm. The powders were then pressed at 100 MPa into disk-shaped compacts 12 mm in diameter and 2–3 mm in thickness on a Carver Model C manual laboratory press (United States). The powder synthesis reaction by-product (ammonium nitrate) and the sodium salts added acted as a temporary process binder. The green powder compacts were fired in a furnace at different temperatures in the range 700–1100°C (heating rate of 5°C/min, holding at the required temperature for 2 h) and then furnace-cooled.

The linear shrinkage and geometric density of the ceramic samples were determined by measuring their mass and dimensions (with an accuracy of ±0.05 mm) before and after firing.

The phase composition of the as-prepared powder, the powder mixtures after disaggregation and homog-

Table 1. Calculated compositions of powder mixtures in which the amount of sodium salts corresponds to 10 mol % Na_2O in the Na_2O–CaO–P_2O_5 phase diagram

No.	Components of the powder mixtures, mol %				The line in the Na_2O–CaO–P_2O_5 system on which the point corresponding to the composition of the mixture is placed
	$CaHPO_4$	$Na_2CO_3 \cdot H_2O$	$Na_4P_2O_7 \cdot 10H_2O$	$(NaPO_3)_n$	
1	100	–	–	–	CaO–P_2O_5
2	94.6	5.4	–	–	$Ca_2P_2O_7$–Na_2O
3	92.3	–	7.7	–	$Ca_2P_2O_7$–$Na_4P_2O_7$
4	89.5	–	–	10.5	$Ca_2P_2O_7$–$NaPO_3$

Table 2. Phase compositions of the powders before and after disaggregation and the ceramics after firing

No.	Composition of the powder before disaggregation	Composition of the powder used for compaction	Composition of the ceramic	
			700–1000°C	1100°C
1	$CaHPO_4$ $CaHPO_4 \cdot 2H_2O$ NH_4NO_3	$CaHPO_4$ NH_4NO_3	β-$Ca_2P_2O_7$	
2	$CaHPO_4$ $CaHPO_4 \cdot 2H_2O$ NH_4NO_3 $Na_2CO_3 \cdot H_2O$	$CaHPO_4 \cdot 2H_2O$ NH_4NO_3	β-$NaCaPO_4$, β-$Ca_2P_2O_7$	
3	$CaHPO_4$ $CaHPO_4 \cdot 2H_2O$ NH_4NO_3 $Na_4P_2O_7 \cdot 10H_2O$	$CaHPO_4 \cdot 2H_2O$ NH_4NO_3	β-$Ca_2P_2O_7$, $Na_2CaP_2O_7$	β-$Ca_2P_2O_7$, $Ca_{10}Na(PO_4)_7$
4	$CaHPO_4$ $CaHPO_4 \cdot 2H_2O$ NH_4NO_3 $(NaPO_3)_n$	$CaHPO_4$ $CaHPO_4 \cdot 2H_2O$ NH_4NO_3	β-$Ca_2P_2O_7$	

enization, and the heat-treated samples was determined by X-ray diffraction on a Rigaku D/Max-2500 rotating-anode diffractometer (Japan) with CuK_α radiation. The phases present were qualitatively identified using ICDD PDF2 database resources [12].

The samples were characterized by simultaneous thermal analysis at a heating rate of 10°C/min, using a Netzsch STA 409 PC Luxx thermoanalytical system (Netzsch, Germany). The sample weight was at least 10 mg. The composition of the vapor phase resulting from the decomposition of the samples was determined using a QMS 403C Aëolos quadrupole mass spectrometer (Netzsch, Germany), combined with the Netzsch STA 409 PC Luxx thermoanalytical system. Mass spectra were taken for the mass numbers 18 (H_2O), 17 (OH/NH_3), 15 (NH), 30 (NO), and 44 (CO_2).

Particle size distributions were obtained using an Analysette 22 MicroTec plus analyzer (Fritsch, Germany).

The microstructures of the samples were examined by scanning electron microscopy on a LEO SUPRA 50 VP electron microscope (Carl Zeiss, Germany; field emission source) at accelerating voltages from 3 to 20 kV in secondary electron imaging mode (SE2 detector). A chromium layer (≤10 nm in thickness) was grown on the sample surface by sputter deposition.

RESULTS AND DISCUSSION

According to X-ray diffraction data, the as-prepared powder consisted of a mixture of brushite and ammonium nitrate. After drying in air at room temperature for a week and then in a drying oven at 40°C for 2 h, the phase composition of the powder was dominated by monetite. In addition, after drying the syn-

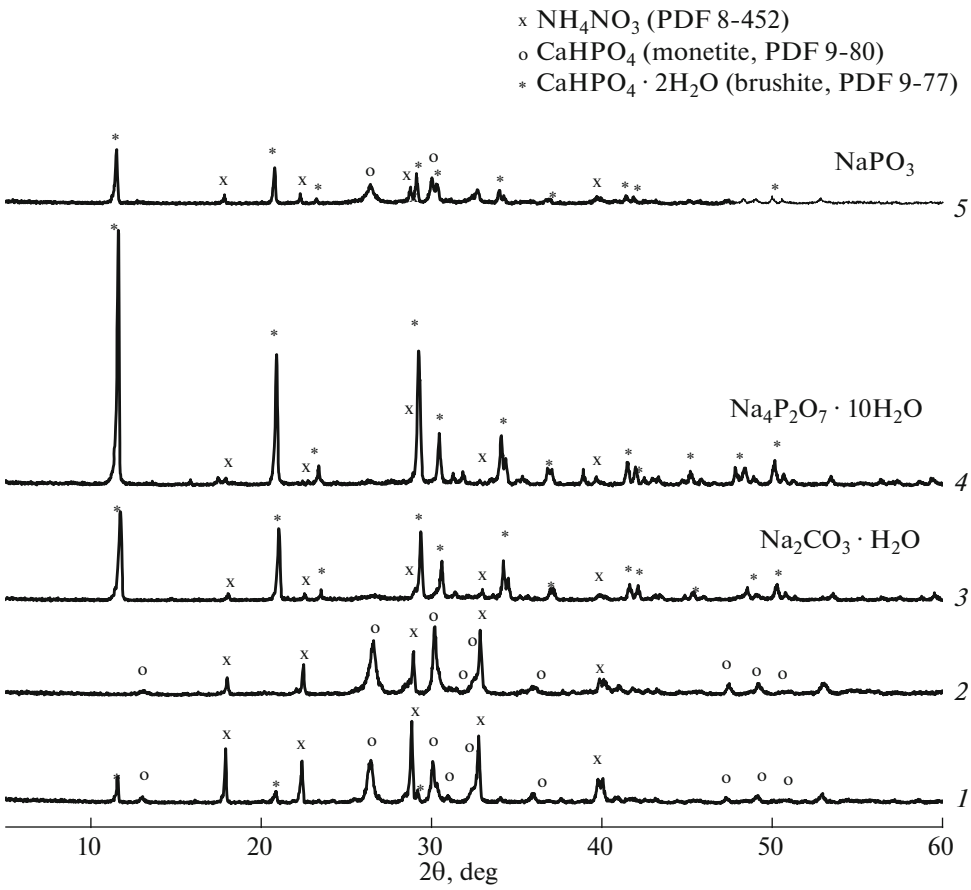

Fig. 2. X-ray diffraction patterns of the synthesized powder after drying (*1*) and disaggregation (*2*) and the sodium salt-containing powder mixtures after disaggregation and homogenization under acetone using mechanical activation in a planetary mill (*3*–*5*).

thesized powder contained some amounts of brushite and ammonium nitrate. The preparation of the powders or powder mixtures for the ceramic fabrication process included the disaggregation of the synthesized powder after drying and the homogenization of the powder mixtures in order to ensure a uniform distribution of their components. These steps were conducted in acetone, a liquid with low surface tension and a relatively low boiling point.

Figure 2 shows X-ray diffraction patterns of the powder mixtures (Table 1) after disaggregation and homogenization in acetone using a planetary mill. After the disaggregation and homogenization, the phase composition of the powder containing no sodium salt additions comprised monetite and ammonium nitrate. In this case, acetone acted as a hygroscopic medium facilitating the dehydration of the relatively small amount of brushite present in the synthesized powder after drying to monetite. After disaggregation, the powder mixtures in which sodium salts were present along with calcium phosphates contained brushite in spite of the disaggregation and homogenization in a hygroscopic liquid (acetone). The reflections from brushite were strongest in the case of the powder mixture containing sodium pyrophosphate decahydrate, $Na_4P_2O_7 \cdot 10H_2O$. In the case of the powder mixture containing sodium carbonate monohydrate, $Na_2CO_3 \cdot H_2O$, the reflections from brushite were slightly weaker. After disaggregation and homogenization, the powder mixtures containing sodium polyphosphate, $(NaPO_3)_n$, consisted of both brushite and monetite. The sodium salts added to the calcium phosphate powder were not detected by X-ray diffraction, which was most likely due to the relatively small amount of the salts (Table 1) in the powder mixture and the transformations caused by mechanical activation in acetone.

In preparing the sodium salt-containing starting powder mixtures for the fabrication of ceramics, monetite rehydration was observed for the first time. Rehydration required water. The most likely water source for the monetite rehydration reaction was water from hydrated salts ($Na_4P_2O_7 \cdot 10H_2O$ and $Na_2CO_3 \cdot H_2O$) or adsorbed water (from X-ray amorphous $(NaPO_3)_n$). Under the conditions of intense mechanical activation of the powder mixtures in acetone, the water was delivered to the disaggregation/homogenization medium. The presence of water during the disaggrega-

tion/homogenization process in acetone ensured conditions for the dissolution and crystallization of calcium hydrogen phosphates (brushite and monetite). This assumption is supported by the fact that the reflections from brushite were strongest when the salt containing the largest amount of water of crystallization ($Na_4P_2O_7 \cdot 10H_2O$) was added. Moreover, in each starting mixture, after drying the synthesized powder contained an amount of brushite, whose particles could act as crystallization centers for this mineral during the dissolution and crystallization processes. Under ordinary conditions, because of the higher water solubility of brushite (0.088 g/L at 25°C) in comparison with monetite (0.048 g/L at 25°C) [13], monetite rehydration to brushite appears unlikely. The brushite phase is metastable and its precipitation from supersaturated salt solutions is caused by kinetic factors.

For monetite rehydration to brushute, three conditions should be fulfilled: (1) the solution pH should be maintained in the stability range of the brushite phase: pH ~ 2–5; (2) there should be brushite seeds, which reduce the energy barrier of nucleation; and (3) the monetite-containing solution should be supersaturated with respect to brushite.

The first condition is fulfilled owing to the presence of NH_4NO_3 (Table 2), whose hydrolysis produces a necessary acid medium. The second condition is also fulfilled because all of the mixtures contained residual brushite. The formation of a local supersaturated solution, from which brushite can be precipitated (third condition) during the mechanical activation of a monetite suspension, can be facilitated by phenomena that take place in the impact zone of a grinding medium, such as elastic deformation of a monetite crystal, its plastic deformation and disintegration, and local adiabatic heating of the solution.

The thermodynamics of a nonhydrostatically stressed solid surrounded by fluid was studied systematically beginning from J. Gibbs, with application to rock metamorphism [14] and also in mechanochemistry in relation to the effect on surface tension on a solid–fluid interface [15]. According to Riecke's principle in geology, plastic deformation and disintegration of a crystal when rock is brought in contact with a grinding medium in the presence of fluid are favorable for reprecipitation from mechanically stressed contact regions between crystals [14]. Local pulsed adiabatic heating is another condition for a nonequilibrium process in which a substance can transform from a more stable phase into a less stable one and then persist in such a form. To date, we have found no reports mentioning monetite rehydration. We think, however, that there are no fundamental factors preventing such a process from taking place during mechanical activation of acid monetite suspensions containing brushite seeds.

Figure 3 shows micrographs of the synthesized powder after drying (Fig. 3a) and the powder mixtures after disaggregation and homogenization in acetone (Figs. 3b–3d). The as-prepared powder consists of platelike particles 1–3 μm in lateral size and 100–300 nm in thickness (Fig. 3a). After disaggregation in acetone, the powder, converted into monetite, consists of aggregates 2–4 μm in size. The aggregates, in turn, consist of needle-like particles. After disaggregation and homogenization in acetone in the presence of calcium carbonate monohydrate, the particles of the rehydrated brushite powder have the form of ribbons 100–500 nm in width and up to 10 μm in length. The formation of similar ribbonlike particles was observed in the process of brushite powder disaggregation in the presence of sodium nitrate [16]. However, in that case, disaggregation was accompanied by brushite dehydration and after the disaggregation the powder consisted of monetite. The particles of the rehydrated monetite obtained in the presence of sodium pyrophosphate decahydrate have platelike morphology characteristic of brushite (Fig. 3d) and are 1–3 μm in lateral size and 200–500 nm in thickness. After disaggregation and homogenization in the presence of sodium polyphosphate, the powder particles contain platelike particles 2–5 μm in size, covered with needle-like particles ranging in size up to 100 nm. The electron microscopy data for the as-prepared powder and the powders after disaggregation and homogenization agree with the X-ray diffraction data.

Thus, traditionally utilized in the technology of ceramics, the disaggregation and homogenization of powder mixtures take a new meaning due to the specific features of the chemical nature of the components used in this study (calcium hydrogen phosphates, sodium pyrophosphate decahydrate, sodium polyphosphate, and sodium carbonate monohydrate) as precursors to high-temperature phases. In the case of the powder mixtures studied here, mechanical activation in acetone can be thought of as not only homogenization of components and disaggregation of the synthesized calcium phosphate powder but also a process that ensures changes in the phase composition and morphology of the calcium phosphate particles as a result of a unique phenomenon: the formation of rehydrated brushite from monetite.

Figure 4 shows the size distribution of aggregates in the powders prepared using mechanical activation. The most probable aggregate size in the powder mixture prepared with the addition of $Na_4P_2O_7 \cdot 10H_2O$ is the smallest: 3.6 μm. The most probable aggregate size in the powder mixture prepared with the addition of $Na_2CO_3 \cdot H_2O$ is the largest: 11.8 μm. The most probable aggregate sizes in the additive-free powder and the powder mixture prepared with the addition of $NaPO_3$ differ little: 4.9 and 5.2 μm, respectively. The particle size distributions correlate with the microstructure of the powders obtained after disaggregation and homogenization. Clearly, the particles with ribbonlike morphology tend to form loose but relatively

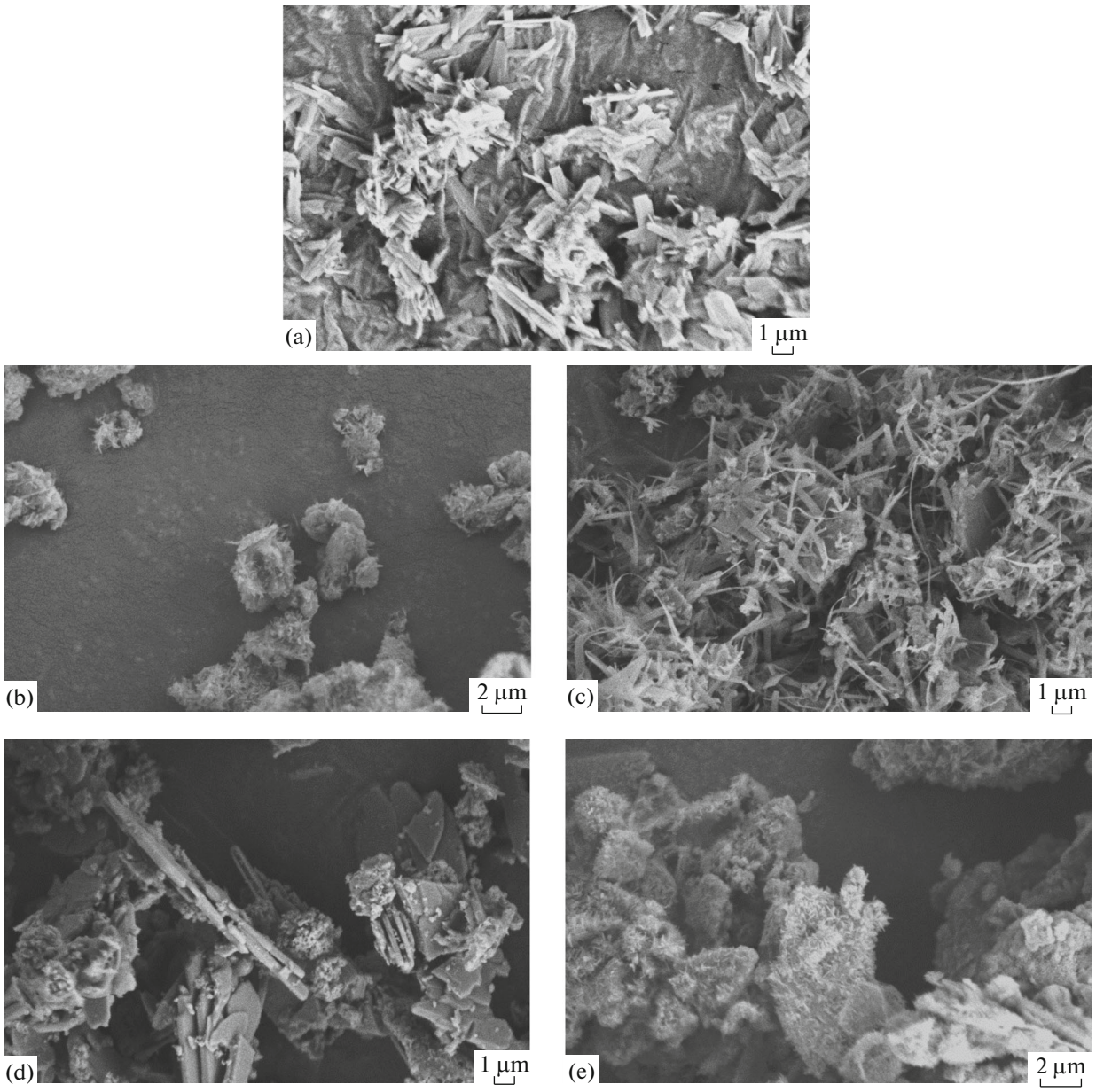

Fig. 3. Micrographs of the calcium phosphate powder after synthesis and drying before (a) and after (b) disaggregation in acetone and the powder mixtures containing $Na_2CO_3 \cdot H_2O$ (c) , $Na_4P_2O_7 \cdot 10H_2O$ (d), and $NaPO_3$ (e) after disaggregation and homogenization in acetone using mechanical activation in a planetary mill.

large aggregates. Primary aggregates, consisting of needle-like particles (additive-free powder) or aggregates of platelike particles covered with needle-like particles (powder prepared with the addition of $NaPO_3$), tend to form secondary aggregates.

The loose bulk density of the powders after disaggregation and homogenization reflects the rheological properties of the powders and their densification behavior. The powders after disaggregation and homogenization are similar in loose bulk density, which lies in the range 0.30–0.34 g/cm^3. The powders in which particles with ribbonlike or platelike morphology prevail have a higher loose bulk density (0.33–0.34 g/cm^3) and, accordingly, have a stronger tendency toward densification than do the aggregates of needle-like particles (0.30–0.31 g/cm^3).

Figure 5 presents thermal analysis data. The powders whose phase composition (Fig. 2) after disaggregation, homogenization, and rehydration is represented by brushite and ammonium nitrate according to X-ray diffraction data have similar thermogravimetric curves obtained during heating to 400°C (Fig. 5a). The curves contain steps due to the removal of physically bound water (near 100°C), ammonium nitrate

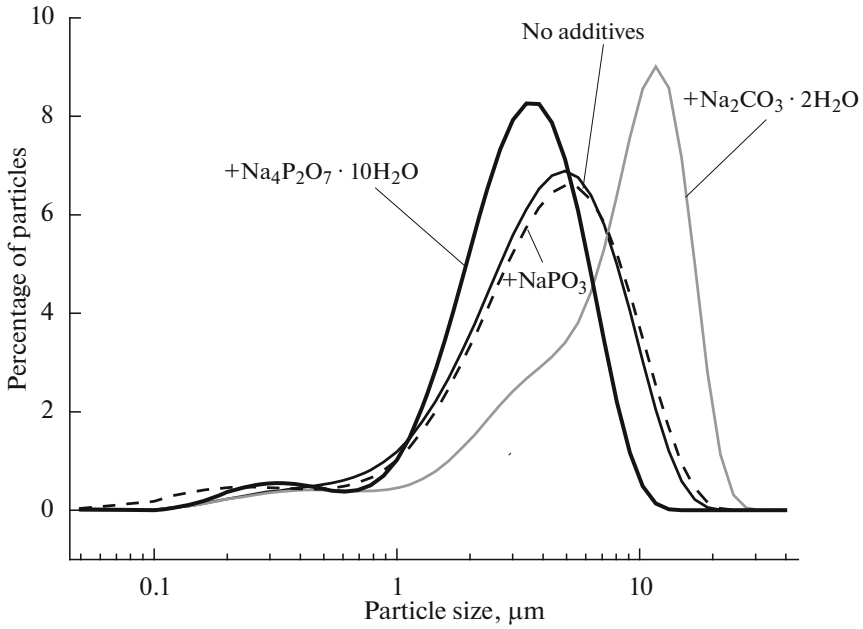

Fig. 4. Particle size distributions of the powders after disaggregation and homogenization in acetone using mechanical activation in a planetary mill.

decomposition, and the transformation of brushite into monetite (near 200°C):

$$CaHPO_4 \cdot 2H_2O = CaHPO_4 + 2H_2O. \quad (2)$$

At higher temperatures, the weight loss curve of the powder mixture containing $Na_2CO_3 \cdot H_2O$ has a step characteristic of monetite, which reflects the transformation of monetite into calcium pyrophosphate at 400°C:

$$2CaHPO_4 = Ca_2P_2O_7 + H_2O. \quad (3)$$

The weight loss curve of the powder mixture containing $Na_4P_2O_7 \cdot 10H_2O$ has no such step, and the sample weight decreases monotonically. It is reasonable to assume that the reaction involved follows the scheme

$$Na_4P_2O_7 + 2CaHPO_4 = 2Na_2CaP_2O_7 + H_2O. \quad (4)$$

Another distinction is that the total weight loss of the powder mixture containing $Na_4P_2O_7 \cdot 10H_2O$ is 45.5%, whereas that of the powder mixture containing $Na_2CO_3 \cdot H_2O$ is 26.5%. A major contribution (15%) to the difference is, most likely, made by the considerable amount of water adsorbed by the powder mixture containing $Na_4P_2O_7 \cdot 10H_2O$. According to mass spectrometry data, the temperature dependence of the ion current (at $m/Z = 44$, which corresponds to CO_2) for the powder mixture containing $Na_2CO_3 \cdot H_2O$ has small peaks near 100 and 400°C and near the melting point of Na_2CO_3 (852°C). The following reaction may occur on heating:

$$Na_2CO_3 + 2CaHPO_4 = 2NaCaPO_4 + H_2O + CO_2. \quad (5)$$

The additive-free powder and the powder mixture prepared with the addition of $NaPO_3$ are similar in total weight loss: 26–27%. Note that the thermogravimetric curve of the powder consisting of monetite and ammonium nitrate has two steps, corresponding to ammonium nitrate decomposition (near 200°C) and the transformation of monetite into calcium pyrophosphate (near 400°C). The weight loss curve of the powder mixture prepared with the addition of $NaPO_3$ shows no weight changes above 250°C. It is reasonable to assume that the events below this temperature were the removal of physically bound water and the transformations of brushite into monetite and monetite into calcium pyrophosphate. Mass spectrometry data demonstrate that the ion current curves for $m/Z = 18$, 17, 15, and 30 have peaks at 250°C, which point to the release of water, ammonia, and nitrogen oxides. The H_2O–$NaPO_3$ phase diagram [17] indicates that, at low water contents (below 25 mol %) and temperatures under 169°C, the system contains $Na_2H_2P_2O_7$ and NaH_2PO_4. The physically bound water and water crystallization from brushite could create conditions for the formation of these compounds. Above 240°C [18], anhydrous phosphates are formed.

According to X-ray diffraction data (Table 2), after test firing over the entire temperature range studied (700–1100°C) the phase composition of ceramics pre-

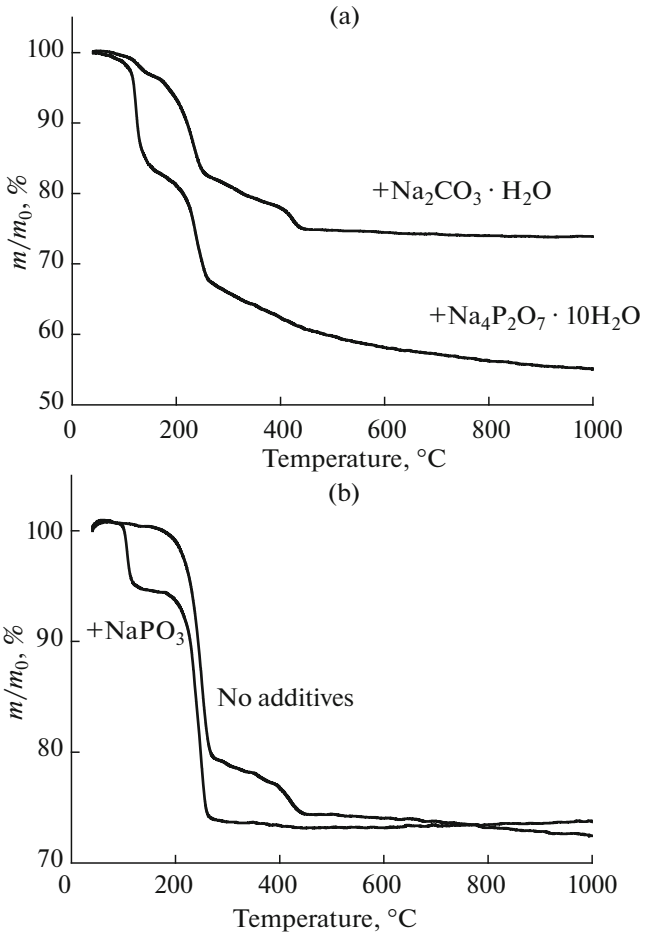

Fig. 5. Thermal analysis data for the powders whose phase composition included (a) brushite and (b) monetite after disaggregation and homogenization.

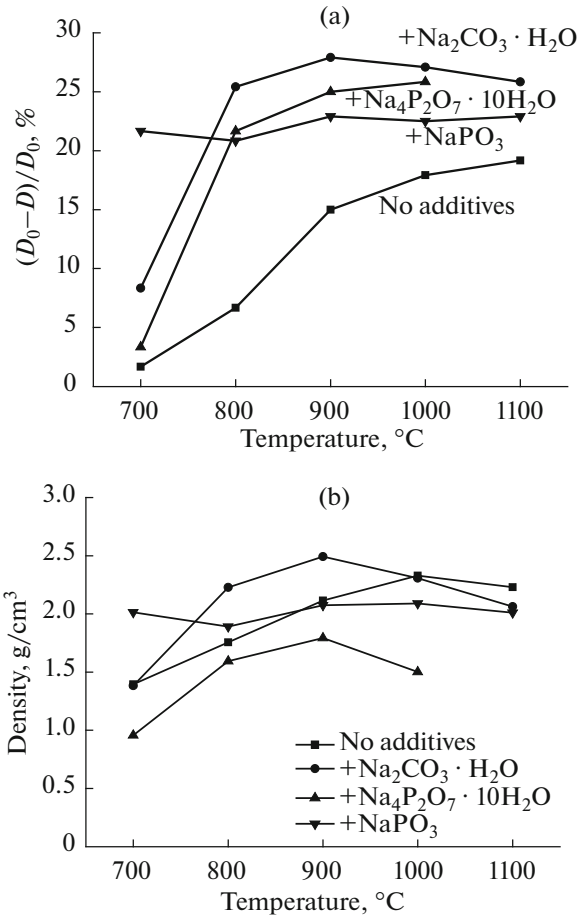

Fig. 6. (a) Linear shrinkage and (b) density of the samples as functions of firing temperature.

pared from the powder containing no sodium salt additions was represented by β-$Ca_2P_2O_7$. Brushite and monetite are direct precursors to the calcium pyrophosphate phase and are formed by reactions (2) and (3).

After test firing over the entire temperature range studied (700–1100°C), the phase composition of ceramics produced from the powder mixture prepared with the addition of $Na_2CO_3 \cdot H_2O$ comprised β-$NaCaPO_4$ and β-$Ca_2P_2O_7$. In this powder mixture, brushite was a direct precursor to calcium pyrophosphate, and the rhenanite phase resulted from the heterogeneous reaction (5).

After test firing in the temperature range 700–1000°C, the phase composition of ceramics produced from the powder mixture prepared with the addition of $Na_4P_2O_7 \cdot 10H_2O$ comprised β-$Ca_2P_2O_7$ and $Na_2CaP_2O_7$. In this powder mixture, brushite was a direct precursor to calcium pyrophosphate, and the sodium calcium double pyrophosphate phase resulted from the heterogeneous reaction (4). The phase composition of the sample from this mixture, which melted after firing at 1100°C, comprised β-$Ca_2P_2O_7$ and $Ca_{10}Na(PO_4)_7$. The melting point of $Na_2CaP_2O_7$ is 1019°C. Molten sodium calcium phosphate glasses have high vapor pressure. This was responsible for the formation of $Ca_{10}Na(PO_4)_7$ in the sample. Moreover, part of the components might be present in the melt and was not detected by X-ray diffraction.

After test firing over the entire temperature range studied (700–1100°C), the phase composition of ceramics produced from the powder mixture prepared with the addition of $NaPO_3$ was represented by β-$Ca_2P_2O_7$. The melting point of sodium polyphosphate, whose amount is not very large, is 625°C. It is most likely for this reason that this phase cannot be detected by X-ray diffraction in the composition of the ceramic samples.

The phase composition of ceramic materials produced from the powder mixtures containing precursors to calcium pyrophosphate ($CaHPO_4$ and $CaHPO_4 \cdot 2H_2O$), sodium oxide ($Na_2CO_3 \cdot H_2O$), sodium pyrophosphate ($Na_4P_2O_7 \cdot 10H_2O$), and sodium polyphosphate ($(NaPO_3)_n$) corresponded to the intended phase composition. The points located on the lines $CaO–P_2O_5$

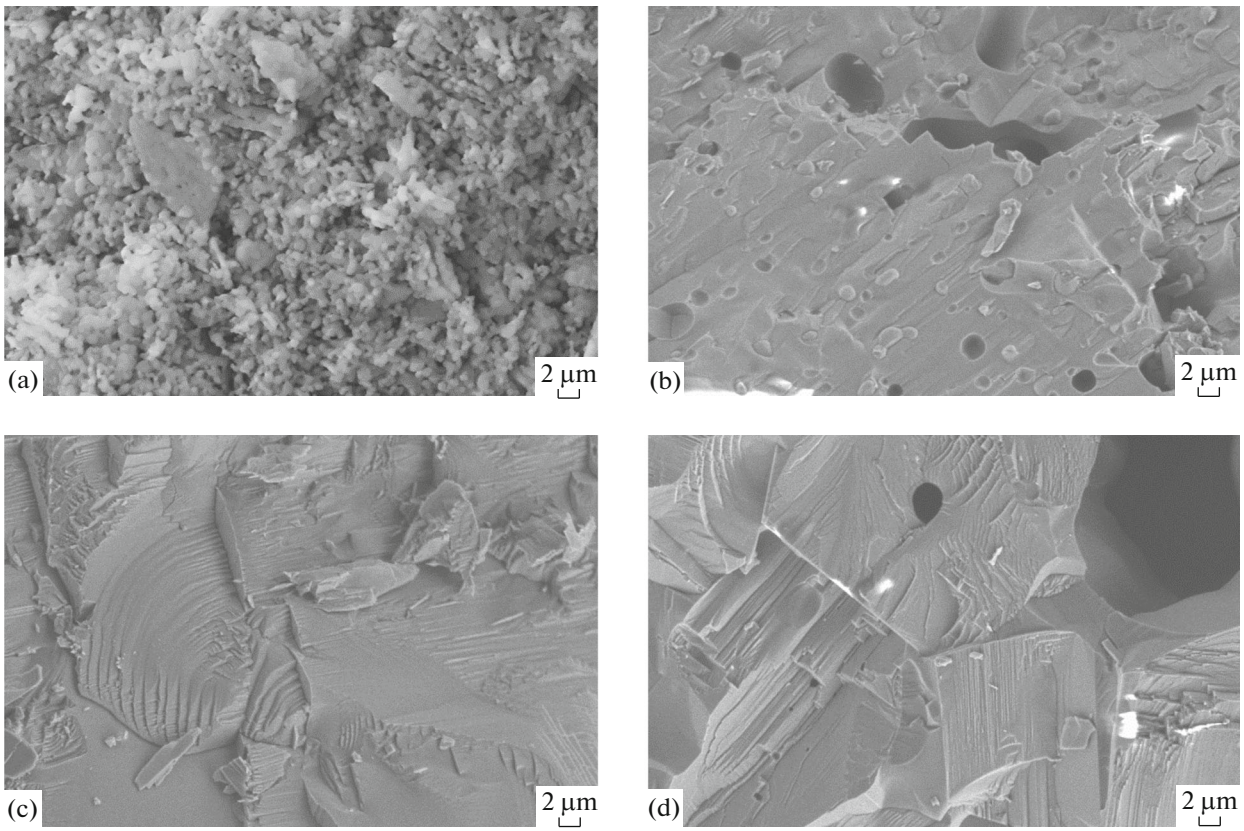

Fig. 7. Microstructures of the ceramics produced from calcium phosphate powders containing no additions (a) and containing the sodium salts $Na_2CO_3 \cdot H_2O$ (b), $Na_4P_2O_7 \cdot 10H_2O$ (c), and $NaPO_3$ (d) after firing at 1000°C.

(point 1), $Ca_2P_2O_7$–Na_2O (point 2), $Ca_2P_2O_7$–$Na_4P_2O_7$ (point 3), and $Ca_2P_2O_7$-$NaPO_3$ (point 4) fall in the region defined by the compounds $Ca_2P_2O_7$, $NaCaPO_4$, $Na_2CaP_2O_7$, and $Ca(PO_3)_2$ in the Na_2O–CaO–P_2O_5 phase diagram.

Figure 6 shows the linear shrinkage (Fig. 6a) and density (Fig. 6b) of the ceramic samples after firing. The maximum linear shrinkage of the ceramic produced from the powder containing no sodium salt additions was 19%, and its density at 1100°C was 2.3 g/cm^3. The relatively low linear shrinkage and density are due to the low diffusion mobility of the pyrophosphate ion.

The maximum linear shrinkage of the ceramic produced from the powder mixture prepared using $Na_2CO_3 \cdot H_2O$ was 28%, and its density at 900°C was 2.5 g/cm^3. After disaggregation and homogenization, the powder mixture consisted of brushite, ammonium nitrate, and Na_2CO_3 formed from $Na_2CO_3 \cdot H_2O$. In examining the formation of a ceramic material, one should take into account that the intended composition falls in the binary system $Ca_2P_2O_7$–$NaCaPO_4$, which lies on the $Ca_2P_2O_7$–Na_2O line; that the powder system contains Na_2CO_3; and that the $Ca_2P_2O_7$–$NaCaPO_4$ line bounds the $NaCaPO_4$–$Ca_2P_2O_7$–$Na_2CaP_2O_7$ region. The $Ca_2P_2O_7$–$NaCaPO_4$ system contains a eutectic (t = 1202°C). The melting point of Na_2CO_3 is 852°C. The $NaCaPO_4$–$Ca_2P_2O_7$–$Na_2CaP_2O_7$ phase field contains binary eutectics in the systems $NaCaPO_4$–$Na_2CaP_2O_7$ (t = 800°C) and $Ca_2P_2O_7$–$Na_2CaP_2O_7$ (t = 803°C). There is also a ternary eutectic, at t = 780°C. Since the maximum changes in shrinkage and density are observed after firing at 800°C, it is reasonable to assume that it is the formation of a eutectic melt at t = 780°C which plays a key role in the densification of the green powder compacts during firing.

The maximum linear shrinkage of the ceramic produced from the powder mixture prepared using $Na_4P_2O_7 \cdot 10H_2O$ was 26% at 1000°C, and its maximum density was 1.8 g/cm^3 at 900°C. The melting point of $Na_2CaP_2O_7$, which forms in this sample during heating, is 1019°C. The $Ca_2P_2O_7$–$Na_2CaP_2O_7$ system contains a eutectic (t = 803°C). This is the only sample that melted after firing at 1100°C.

After firing in the range 700–1100°C, the linear shrinkage of the ceramic produced from the powder mixture prepared using $(NaPO_3)_n$ was 21–23% and its density was 1.9–2.1 g/cm^3. The density and shrinkage data suggest that the densification processes in this sample reached completion at temperatures below

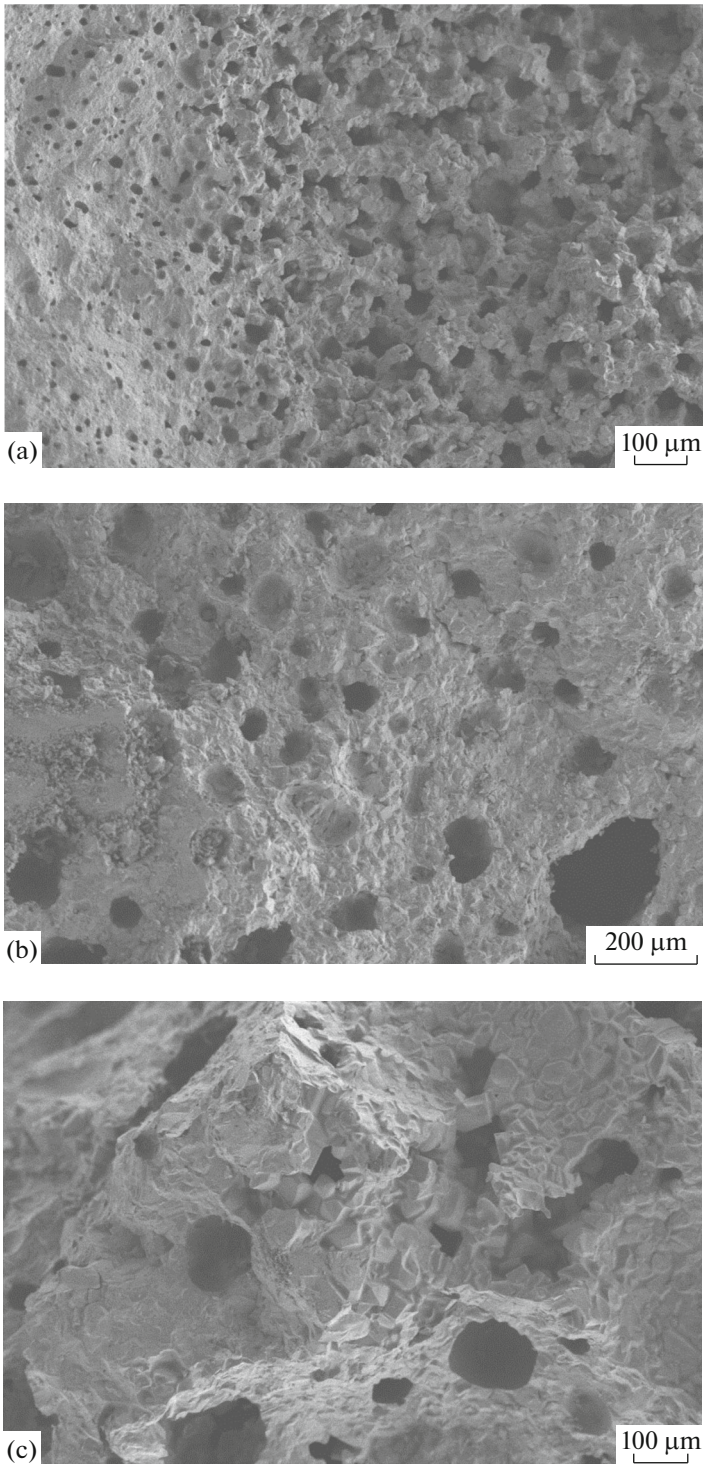

Fig. 8. Microstructures of the ceramics produced from the calcium phosphate powder containing $Na_4P_2O_7 \cdot 10H_2O$ after firing at (a) 800, (b) 900, and (c) 1000°C.

700°C, given that the melting point of $NaPO_3$ is 625°C.

The ceramics based on the sodium salt-containing powder mixtures have a higher linear shrinkage than does the ceramic produced from the additive-free calcium phosphate powder. This is most likely due to melt formation in the samples. Compositions 2–4 (Fig. 1) of the ceramic materials lie in a region in the Na_2O–CaO–P_2O_5 phase diagram that contains a number of eutectics and components with low melting points, so a

melt can be formed in the samples at temperatures above 625°C. For example, the β-$NaCaPO_4$–β-$Ca_2P_2O_7$ system contains a eutectic at t = 1202°C and about 30 wt % $NaCaPO_4$. Moreover, sodium carbonate (a component of the powder mixture) has t_m = 852°C. The $NaCaPO_4$–$Ca_2P_2O_7$–$Na_2CaP_2O_7$ composition triangle contains a ternary eutectic at t = 780°C and binary eutectics in the systems $NaCaPO_4$–$Na_2CaP_2O_7$ (t = 800°C) and $Ca_2P_2O_7$–$Na_2CaP_2O_7$ (t = 803°C). The lower density of the samples after firing at a temperature of 1000°C is most likely due to the release of volatile components from the melts forming in the samples.

Figure 7 illustrates the microstructures of the ceramics with compositions 1–4 (indicated in Fig. 1) after firing at 1000°C. The ceramic containing no sodium salt additions (Fig. 7a) appears not sintered. The grain size is 1–2 μm. The microstructure of the ceramics based on the powder mixtures containing sodium salts is characterized by conchoidal fracture and intragranular porosity. The conchoidal fracture suggests the presence of a considerable amount of a melt during sintering. The presence of a melt provokes anomalous grain growth processes through the dissolution/crystallization mechanism. We believe that the spherical shape of the pores is the consequence of the coalescence of melt droplets, whose viscosity prevents gas bubbles from leaving the droplets.

Figure 8 illustrates the microstructures of the ceramic produced from the mixture prepared using $Na_4P_2O_7 \cdot 10H_2O$, after firing at different temperatures. It can be seen in the micrographs that, as the firing temperature is raised from 800 to 1000°C, the pore size increases and the number of pores drops. At a lower magnification, the grain size in the ceramic can be evaluated. At 1000°C, the grain size is 30–100 μm. The anomalous grain growth is due to the presence of a melt, which creates conditions for the dissolution/crystallization process.

CONCLUSIONS

Ceramic materials in the Na_2O–CaO–P_2O_5 system have been produced using powder mixtures containing calcium hydrogen phosphates ($CaHPO_4$/$CaHPO_4 \cdot 2H_2O$) and sodium salts ($Na_2CO_3 \cdot H_2O$, $Na_4P_2O_7 \cdot 10H_2O$, and $NaPO_3$). The mechanical activation of these mixtures in acetone, intended to disaggregate the synthesized calcium hydrogen phosphate and homogenize their components, led to partial (in the presence of $NaPO_3$) or complete (in the presence of $Na_2CO_3 \cdot H_2O$ and $Na_4P_2O_7 \cdot 10H_2O$) monetite rehydration to brushite. After the mechanical activation, the powder mixtures contained direct precursors to the calcium pyrophosphate ($Ca_2P_2O_7$) phase, sodium oxide, sodium pyrophosphate, and sodium polyphosphate. The desired phases of ceramic materials in the $Ca_2P_2O_7$–$NaCaPO_4$–$Na_2CaP_2O_7$–$Ca(PO_3)_2$ region of the Na_2O–CaO–P_2O_5 phase diagram resulted from either thermal conversion ($Ca_2P_2O_7$) or a heterophase reaction ($NaCaPO_4$ and $Na_2CaP_2O_7$). The resultant calcium phosphate-based ceramic composites, containing bioresorbable and biocompatible phases, can be recommended for bone implant fabrication.

ACKNOWLEDGMENTS

This work was supported by the Russian Foundation for Basic Research, grant nos. 16-08-01172 and 16-53-00154.

In this study, we used equipment purchased through the Development of Moscow State University Program.

REFERENCES

1. Danil'chenko, S.N., Structure and properties of calcium apatites from the viewpoint of biomineralogy and biomaterials research (a review), *Visn. Sumsk. Derzh. Univ., Ser. Fiz., Mat., Mekh.,* 2007, no. 2, pp. 33–59.
2. Gerk, S.A. and Golovanova, O.A., Normal and pathological elemental compositions of human bone tissue, *Vestn. Omsk. Univ.,* 2015, no. 4 (78), pp. 39–44.
3. Putlyaev, V.I. and Safronova, T.V., A new generation of calcium phosphate biomaterials: the role of phase and chemical compositions, *Glass Ceram.,* 2006, vol. 63, nos. 3–4, pp. 99–102.
4. Barinov, S.M., Calcium phosphate-based ceramic and composite materials for medicine, *Russ. Chem. Rev.,* 2010, vol. 79, no. 1, pp. 13–29.
5. Jones, J.R., Review of bioactive glass: from Hench to hybrids, *Acta Biomater.,* 2015, no. 5, pp. 553–582.
6. Knowles, J.C., Phosphate based glasses for biomedical applications, *J. Mater. Chem.,* 2003, vol. 13, no. 10, pp. 2395–2401.
7. Stroganova, E.E., Mikhailenko, N.Yu., and Moroz, O.A., Glass-based biomaterials: present and future (a review), *Glass Ceram.,* 2003, vol. 60, nos. 9–10, pp. 315–319.
8. Millet, J.M., Sassoulas, R., and Sebaoun, A., Transitions solide ⇌ solide dans le systeme CaO–Na_2O–P_2O_5; sous-systeme $Ca_3(PO_4)_2$–$CaNaPO_4$, *J. Therm. Anal.,* 1983, vol. 28, no. 1, pp. 131–146.
9. Berak, J. and Znamierowska, T., Phase equilibria in the system CaO–Na_2O–P_2O_5. Part II. The partial system $Ca(PO_3)_2$–Na_2O–P_2O_5, *Rocz. Chem.,* 1972, vol. 46, no. 10, pp. 1697–1708.
10. Znamierowska, T., Phase equilibriums in the system calcium oxide–potassium oxide–phosphorus(V) oxide. Part II. Partial system calcium phosphate–calcium potassium pyrophosphate–potassium metaphosphate–calcium pyrophosphate, *Pol. J. Chem.,* 1978, vol. 52, no. 6, pp. 1127–1134.

11. Safronova, T.V. and Putlyaev, V.I., Powder systems for calcium phosphate ceramics, *Inorg. Mater.,* 2017, vol. 53, no. 1, pp. 17–26.

12. PDF4+ Database, Soorya Kabekkodu, Ed., Newtown Square: International Centre for Diffraction Data, 2010. http://www.icdd.com/products/pdf2.htm.

13. Dorozhkin, S.V., Calcium orthophosphates and human beings: a historical perspective from the 1770s until 1940, *Biomatter,* 2012, vol. 2, no. 2, pp. 53–70.

14. Ostapenko, G.T., *Termodinamika negidrostaticheskikh sistem i ee primenenie v teorii metamorfizma* (Thermodynamics of Nonhydrostatic Systems and Its Application in Metamorphism Theory), Kiev: Naukova Dumka, 1977.

15. Rusanov, A.I., *Termodinamicheskie osnovy mekhanokhimii* (Thermodynamic Principles of Mechanochemistry), Moscow: Nauka, 2006.

16. Safronova, T.V., Putlyaev, V.I., Filippov, Ya.Yu., Shatalova, T.B., and Fatin, D.S., Ceramics based on brushite powder synthesized from calcium nitrate and disodium and dipotassium hydrogen phosphates, *Inorg. Mater.,* 2018, vol. 54, no. 2, pp. 195–207.

17. Morey, G.W., The system H_2O–$NaPO_3$, *J. Am. Chem. Soc.,* 1953, vol. 75, no. 23, pp. 5794–5797.

18. Schrödter, K., Bettermann, G., Staffel, T., Wahl, F., Klein, T., and Hofman, T., Phosphoric acid and phosphates, in *Ullmann's Encyclopedia of Industrial Chemistry,* 2008.

Translated by O. Tsarev